

Calculation of Two-Loop Self-Energies in the electroweak Standard Model¹

S. BAUBERGER, M. BÖHM, G. WEIGLEIN²

*Institut für Theoretische Physik, Universität Würzburg
Am Hubland, D-97074 Würzburg, Germany*

F.A. BERENDS, M. BUZA

*Instituut-Lorentz, University of Leiden
P.O.B. 9506, 2300 RA Leiden, The Netherlands*

Abstract:

Motivated by the results of the electroweak precision experiments, studies of two-loop self-energy Feynman diagrams are performed. An algebraic method for the reduction of all two-loop self-energies to a set of standard scalar integrals is presented. The gauge dependence of the self-energies is discussed and an extension of the pinch technique to the two-loop level is worked out. It is shown to yield a special case of the background-field method which provides a general framework for deriving Green functions with desirable theoretical properties. The massive scalar integrals of self-energy type are expressed in terms of generalized multivariable hypergeometric functions. The imaginary parts of these integrals yield complete elliptic integrals. Finally, one-dimensional integral representations with elementary integrands are derived which are well suited for numerical evaluation.

INLO-PUB-11/94

June 1994

¹To appear in Nucl. Phys. B (Proceedings Supplements)

²E-mail address: weiglein@vax.rz.uni-wuerzburg.d400.de

Calculation of two-loop self-energies in the electroweak Standard Model* †

S. Bauberger,^aF.A. Berends,^bM. Böhm,^a M. Buza^b and G. Weiglein^a

^aInstitut für Theoretische Physik, Universität Würzburg, Am Hubland, D-97074 Würzburg, Germany

^bInstituut-Lorentz, University of Leiden, P.O.B. 9506, 2300 RA Leiden, The Netherlands

Motivated by the results of the electroweak precision experiments, studies of two-loop self-energy Feynman diagrams are performed. An algebraic method for the reduction of all two-loop self-energies to a set of standard scalar integrals is presented. The gauge dependence of the self-energies is discussed and an extension of the pinch technique to the two-loop level is worked out. It is shown to yield a special case of the background-field method which provides a general framework for deriving Green functions with desirable theoretical properties. The massive scalar integrals of self-energy type are expressed in terms of generalized multivariable hypergeometric functions. The imaginary parts of these integrals yield complete elliptic integrals. Finally, one-dimensional integral representations with elementary integrands are derived which are well suited for numerical evaluation.

1. INTRODUCTION

The beautiful results of the LEP experiments [1] have shown that the electroweak theory has a predictive power like QED several decades ago. It is to be expected that eventually the electroweak theory will provide high precision predictions for many experiments in the present and near future. One may in particular think in this respect of the measurement of the Z mass and width, a better determination of the W mass and a direct indication of the top mass.

These developments will require in the future two-loop calculations in the electroweak theory. In the study of the two-loop contributions the self-energy diagrams play a central role. The present paper reviews the problems one encounters when considering self-energies in the Standard Model (SM) and discusses recently developed methods to tackle them.

The choice to treat first the self-energies is a logical one. They are the simplest two-loop diagrams which yield a universal contribution to all two-loop processes. Moreover, from one-loop

calculations we know their importance. Several results for two-loop self-energies are known, involving however approximations. They concern the limiting cases of a heavy fermion doublet [2], a heavy top quark [3] and a large Higgs mass [4]. However, in the electroweak theory also the W and Z bosons have a non-negligible mass, and one is in general faced with two-loop self-energies containing massive propagators.

Let us summarize the problems which arise when evaluating two-loop self-energies. The first problem is the plethora of Feynman diagrams contributing, the second one the evaluation of tensor integrals in terms of scalar integrals and the third one the calculation of the scalar integrals themselves. When discussing the corrections due to two-loop self-energies, one furthermore has to deal with the problem that these contributions are in general gauge dependent.

In order to handle the large number of Feynman diagrams needed for the evaluation of two-loop self-energies, an algebraic approach is chosen allowing for a high degree of automatization. It involves a method for the decomposition of tensor integrals. Whereas for one-loop diagrams this is a well-known procedure [5], it was only recently developed for two-loop self-energies [6]. In this way all two-loop self-energies can be reduced to a set of standard scalar integrals. The task of

*Combined talks, presented by F.A. Berends, M. Böhm and G. Weiglein at the Zeuthen Workshop on Elementary Particle Theory — Physics at LEP200 and Beyond, held at Teupitz, Germany, April 10–15 1994

†Research supported by EU contract CHRX-CT-92-0004, Stichting FOM and Deutsche Forschungsgemeinschaft

evaluating any two-loop self-energy involving in general several thousands of Feynman amplitudes is therefore reduced to the problem of calculating four different types of two-loop scalar integrals. As an example, we treat light fermion contributions to the self-energy of the Z -boson. The results given in a minimal basis of standard integrals allow to study the gauge dependence of the considered quantities directly at the algebraic level.

At one-loop order the self-energies are frequently used as building blocks to define running couplings or to parametrize electroweak radiative corrections. The need for self-energies as building blocks with suitable theoretical properties seems to be even more important at the two-loop level, where so far no calculation of a complete process exists. In the one-loop applications it was found that the self-energies evaluated in the class of R_ξ -gauges are not adequate as building blocks due to their gauge dependence and unsatisfactory high energy and UV behavior. Many proposals to modify these self-energies aimed on eliminating their gauge parameter dependence. In particular, the pinch technique (PT) [7] was found to yield results with decent properties. Recently it was shown [8] that the background-field method (BFM) [9] offers a wider framework in which Green functions possessing desirable theoretical properties are directly derived from a gauge invariant effective action. In this paper we work out an extension of the PT to the two-loop level and show that it corresponds to a special case of the BFM results.

The evaluation of the two-loop scalar integrals is in general needed for non-negligible masses and an arbitrary dimension D . When expanding around $\delta = (4 - D)/2 \sim 0$, one gets in these cases not anymore results in terms of (poly) logarithms. To perform nevertheless an evaluation of the massive two-loop diagrams, in essence two approaches are followed: expansions for small and large external momenta and numerical integration. In both strategies this paper presents recent new results. On one hand, the use of multi-variable generalized hypergeometric functions, i.e. multiple series, is a new development. On the other hand, one-dimensional integral representations are de-

rived, which are a good alternative to the existing two-dimensional integrals. It turns out that the derivation of one-dimensional integrals is possible for all two-loop diagrams which contain a one-loop self-energy insertion.

For the imaginary parts of the scalar integrals simple analytic results in terms of complete elliptic integrals are derived.

The outline of the paper is as follows.

The algebraic method for reducing two-loop self-energies to standard scalar integrals is described in section 2, whereas in section 3 the question of gauge invariance in the framework of PT and BFM is discussed. The next section deals with an analytic approach to scalar self-energy integrals leading to generalized hypergeometric functions. Section 5 focuses on the imaginary part of the scalar integrals, which are then expressed in terms of elliptic integrals. The one-dimensional integral representations are derived in section 6. In section 7 we give our conclusions and an outlook.

2. ALGEBRAIC CALCULATION OF TWO-LOOP SELF-ENERGIES

2.1. Classification

As the first step in the evaluation of two-loop self-energies, the relevant Feynman diagrams have to be generated. These can be classified according to their topologies. In fig. 1 some examples of irreducible two-loop self-energy topologies are shown. A complete set including also tadpoles and topologies which factorize into one-loop contributions is given in [6]. Inserting fields into the topologies in all possible ways and applying the Feynman rules yields all relevant Feynman amplitudes. The generation of the Feynman diagrams and amplitudes is carried out automatically with the program *FeynArts* [10].

In the following we will use the shorthand notations

$$\langle\langle \dots \rangle\rangle = \int \frac{d^D q_1}{i\pi^2 (2\pi\mu)^{D-4}} \int \frac{d^D q_2}{i\pi^2 (2\pi\mu)^{D-4}} (\dots),$$

where q_1 and q_2 are the integration momenta of the loop integrals and μ is an arbitrary reference

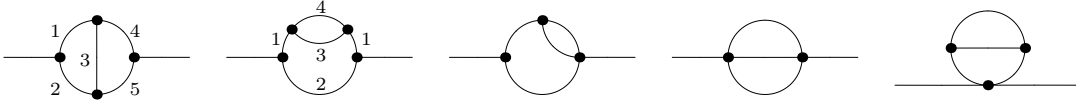


Figure 1. One-particle irreducible topologies of two-loop self-energies.

mass, and

$$d_{ij\dots l} = \frac{1}{\left[k_i^2 - m_i^2\right] \left[k_j^2 - m_j^2\right] \cdots \left[k_l^2 - m_l^2\right]}.$$

Here k_i is the momentum of the i -th propagator and m_i its mass. In the most general case corresponding to the first topology in fig. 1 five different propagators appear. Their momenta are related to the integration momenta q_1 and q_2 and the external momentum p via

$$\begin{aligned} k_1 &= q_1, \quad k_2 = q_1 + p, \quad k_3 = q_2 - q_1, \quad k_4 = q_2, \\ k_5 &= q_2 + p. \end{aligned} \quad (1)$$

A general Feynman amplitude takes the form

$$\langle\langle f(k_i, m_i, D) d_{12\dots l} \rangle\rangle, \quad (2)$$

where $f(k_i, m_i, D)$ is an expression depending on the momenta, the particle masses and the space-time dimension D and containing the whole Lorentz and Dirac structure.

As will be discussed in the next section, all two-loop self-energies can be reduced to a class of standard scalar integrals which we call T -integrals

$$\begin{aligned} T_{i_1 i_2 \dots i_l}(p^2; m_1^2, m_2^2, \dots, m_l^2) &= \\ &= \langle\langle \frac{1}{\left[k_{i_1}^2 - m_1^2\right] \left[k_{i_2}^2 - m_2^2\right] \cdots \left[k_{i_l}^2 - m_l^2\right]} \rangle\rangle, \end{aligned} \quad (3)$$

where the denominator is of the same form as in the Feynman amplitude. The double index notation $T_{i_1 i_2 \dots i_l}$ is used here to indicate that the indices of the T -integrals refer to the corresponding momenta $k_{i_1}, k_{i_2}, \dots, k_{i_l}$. In the following the momentum p^2 and the masses will only be explicitly written as arguments if confusion is possible.

The topologies depicted in fig. 1 correspond to the scalar integrals $T_{12345}, T_{11234}, T_{1234}, T_{234}$ and T_{1134} , respectively. The analytical expression for T_{11234} can be obtained from T_{1234} by partial fractioning or taking the derivative with respect to

m_1^2 . Other integrals with higher powers of propagators are treated in the same way. For the general case one therefore needs to evaluate only four different types of two-loop scalar integrals.

2.2. Reduction to standard scalar integrals

It is convenient to begin with a decomposition into Lorentz scalars. For the gauge boson self-energies it reads

$$\Sigma_{\mu\nu}(p) = \left(-g_{\mu\nu} + \frac{p_\mu p_\nu}{p^2}\right) \Sigma_T(p^2) - \frac{p_\mu p_\nu}{p^2} \Sigma_L(p^2),$$

from which the transverse part $\Sigma_T(p^2)$ and the longitudinal part $\Sigma_L(p^2)$ can be obtained

$$\begin{aligned} \Sigma_T(p^2) &= \frac{1}{D-1} \left(-g^{\mu\nu} + \frac{p^\mu p^\nu}{p^2}\right) \Sigma_{\mu\nu}(p); \\ \Sigma_L(p^2) &= -\frac{p^\mu p^\nu}{p^2} \Sigma_{\mu\nu}(p). \end{aligned}$$

For all other types of self-energies scalar quantities can be extracted in a similar way [6].

The contraction of Lorentz indices, reduction of the Dirac algebra and evaluation of Dirac traces can be worked out like in the one-loop case, e.g. with the program *FeynCalc* [11]. Since we deal with scalar quantities, this results in scalar products of momenta ($k_i \cdot k_j$), ($k_i \cdot p$), p^2 in the numerator of the Feynman amplitude. The denominator is unchanged. We now implicitly use momentum conservation and express all scalar products as sums of momentum squares, e.g.

$$(k_1 \cdot p) = \frac{1}{2}(k_2^2 - k_1^2 - p^2). \quad (4)$$

Subsequently all k_i^2 appearing both in the numerator and the denominator are canceled via

$$k_i^2 = (k_i^2 - m_i^2) + m_i^2. \quad (5)$$

In general there remain k_i^2 in the numerator which cannot be canceled, e.g. for

$$I = \langle\langle k_5^2 d_{1234} \rangle\rangle. \quad (6)$$

We proceed in this case by writing

$$k_5^2 = (k_4^2 - m_4^2) + (m_4^2 + p^2) + 2(p \cdot k_4). \quad (7)$$

The first term can be canceled with the appropriate propagator factor in the denominator. The second term contains no integration momenta. We therefore focus on the integral

$$p_\mu S_{1234}^{4,\mu} = p_\mu \langle (k_4^\mu d_{1234}) \rangle \quad (8)$$

and perform a tensor decomposition for $S_{1234}^{4,\mu}$.

In contrast to the one-loop case the decomposition with respect to the external momentum, i.e. the ansatz [5]

$$S_{1234}^{4,\mu} = p^\mu S(p^2), \quad (9)$$

does not lead to simpler integrals here. In order to determine the scalar quantity $S(p^2)$, one has to contract with p_μ yielding terms in the numerator which cannot be canceled. This fact is due to the structure of the topology associated with $S_{1234}^{4,\mu}$ (the third topology in fig. 1) which contains a four-vertex with three inner lines. This is a typical feature of two-loop topologies not present at the one-loop level.

Instead, we perform a decomposition with respect to a subloop. We write

$$\begin{aligned} \langle k_4^\mu d_{34} \rangle &\equiv \\ &\equiv \int \frac{d^D q_2}{i\pi^2 (2\pi\mu)^{D-4}} \frac{q_2^\mu}{\left[(q_2 - k_1)^2 - m_3^2 \right] \left[q_2^2 - m_4^2 \right]} \\ &= k_1^\mu s(k_1^2), \end{aligned} \quad (10)$$

where the last equality follows from the fact that the tensor integral depends only on k_1^μ . The quantity $s(k_1^2)$ is given by

$$s(k_1^2) = \frac{1}{k_1^2} \langle (k_1 \cdot k_4) d_{34} \rangle = \langle (k_1 \cdot k_4) d_{1'34} \rangle. \quad (11)$$

The factor $1/k_1^2$ can be written as a massless propagator, which we have indicated with a prime at the corresponding index in $d_{1'34}$. Inserting this into (8) yields

$$p_\mu S_{1234}^{4,\mu} = \langle \langle (p \cdot k_1) (k_1 \cdot k_4) d_{1'1234} \rangle \rangle. \quad (12)$$

The scalar products in the numerator of this integral can now be expressed in terms of squared

momenta which can be canceled. Therefore all momentum dependent terms have been removed from the numerator of the Feynman integral while its denominator has retained its original structure. It can further be simplified by performing a partial fractioning for the propagator factors $d_{1'1}$ carrying the same momentum.

It can be shown [6] that in a similar way all possible integrals appearing in calculations of general two-loop self-energies can be reduced to T -integrals.

The result of the algebraic calculation in general contains several scalar integrals depending on different arguments. These are not necessarily independent of each other, i.e. there exist relations

$$c^1 T^1 + c^2 T^2 + \dots + c^n T^n = 0 \quad (13)$$

where c^1, \dots, c^n are polynomials in p^2 . We use these relations together with the symmetry properties of the T -integrals to eliminate as many integrals as possible. This leads to a minimal set of scalar integrals which are algebraically independent of each other. The result expressed in this minimal basis is very transparent and directly displays certain properties of the considered quantity.

For example, Slavnov-Taylor identities can be checked at a purely algebraic level without having to use any explicit expression for the T -integrals. When adding up the results for the relevant amplitudes, the coefficient of every standard integral exactly adds up to zero. This has been demonstrated in [6] for Slavnov-Taylor identities involving several thousands of Feynman amplitudes.

The algorithms outlined here have been implemented into the program *TwoCalc* [12] which carries out the algebraic calculation fully automatically.

2.3. Results for the Standard Model

Another feature which can directly be read off from the algebraic result is its gauge dependence. We work in a general R_ξ -gauge specified by one gauge parameter ξ_i ($i = \gamma, Z, W$) for each vector boson and write the lowest-order gauge boson

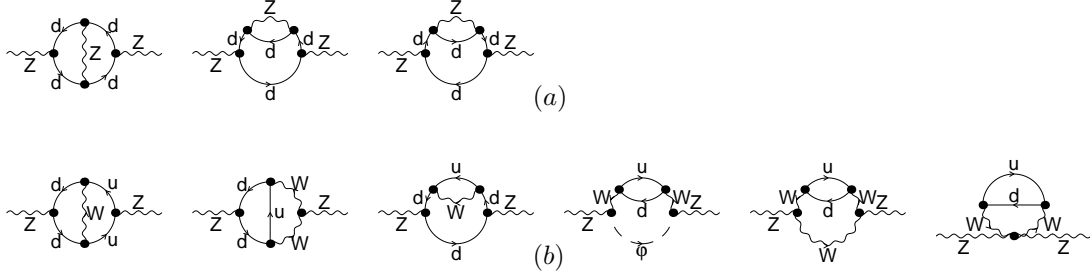


Figure 2. Light fermion contributions to the two-loop self-energy of the Z -boson.

propagators as

$$\Delta_{\mu\nu}^i = \frac{-ig_{\mu\nu}}{[k^2 - m_i^2]} + \frac{i(1 - 1/\xi_i)k_\mu k_\nu}{[k^2 - m_i^2/\xi_i][k^2 - m_i^2]} \quad (14)$$

As a simple example, we consider two sets of light fermion graphs contributing to the Z self-energy. They are shown in fig. 2. A complete listing of the light fermion contributions to the gauge boson self-energies was given in [6]. All fermions except the top-quark can be treated as light fermions, i.e. their masses are small compared to those of the Z - and W -bosons and can therefore be neglected. For definiteness, we choose d - and u -quark.

We find for the transverse part of the three “neutral current” diagrams depicted in fig. 2a

$$\begin{aligned} \Sigma_{T,Z}^{ZZ,(2)}(p^2) = & e^4 C_Z \left[f_Z(A_0, B_0) \right. \\ & + (4 - 6D + D^2)T_{13'4'}(m_Z^2) \\ & + (8 - 4D + D^2)T_{23'4'}(p^2; m_Z^2) \\ & - (4 - 8D + D^2)(m_Z^2 + p^2)T_{1'2'34'}(p^2; m_Z^2) \\ & - D(m_Z^4 + 4m_Z^2 p^2 - m_Z^2 p^2 D/2 + p^4) \\ & \left. \times T_{1'2'34'5'}(p^2; m_Z^2) \right], \quad (15) \end{aligned}$$

whèrè C_Z is a dimensionless constant and $f_Z(A_0, B_0)$ represents a function containing only scalar one-loop integrals. The result for each single diagram of fig. 2a depends on the gauge parameter ξ_Z . However, as is seen in (15), in the sum of these diagrams the gauge parameter has canceled, i.e. this contribution is gauge independent within the class of R_ξ -gauges.

Fig. 2b represents a set of “charged current” diagrams where a W^\pm is exchanged. We have

only drawn one diagram of each type. The result for the altogether 15 amplitudes is given by

$$\begin{aligned} \Sigma_{T,W^\pm}^{ZZ,(2)}(p^2) = & \frac{e^4 C}{m_W^2 m_Z^2} \left[f(A_0, B_0) \right. \\ & + g(A_0, B_0; \xi_W) + F(T) \\ & \left. + 9(p^2 - m_Z^2)(2m_W^2 - m_Z^2 - p^2) \frac{m_W^2}{p^2} G(T; \xi_W) \right]. \quad (16) \end{aligned}$$

Here C is again a dimensionless constant, $f(A_0, B_0)$ and $g(A_0, B_0; \xi_W)$ represent terms which only involve scalar one-loop integrals, and $F(T)$ and $G(T; \xi_W)$ contain the scalar two-loop integrals. In contrast to (15), this result is gauge dependent. For illustration, we only give here the explicit form of the gauge parameter dependent function $G(T; \xi_W)$:

$$\begin{aligned} G(T; \xi_W) = & \frac{1}{\xi_W} (D - 3) T_{13'4'}(m_W^2) \\ & + T_{23'4'}(p^2; m_W^2/\xi_W) \\ & - 2 \left[\left(\frac{1}{\xi_W} - 1 \right) m_W^2 + (3 - 2D)p^2 \right] \\ & \times T_{123'4'}(p^2; m_W^2, m_W^2/\xi_W) \\ & + \left[m_W^4 \left(\frac{1}{\xi_W} - 1 \right)^2 - 2 \left(\frac{1}{\xi_W} + 3 - 2D \right) m_W^2 p^2 \right. \\ & \left. + p^4 \right] T_{1123'4'}(p^2; m_W^2, m_W^2, m_W^2/\xi_W). \quad (17) \end{aligned}$$

The gauge parameter appears both in the arguments of the scalar integrals and in their coefficients. The other terms contributing to (16) were explicitly given in Ref. [6].

The characteristic feature of the result (16) is the factor $(p^2 - m_Z^2)$ multiplying the gauge dependent part $G(T; \xi_W)$ which contains the generic

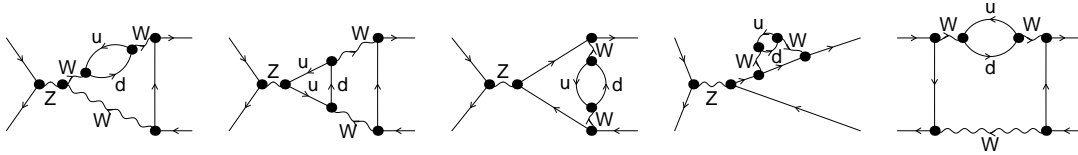


Figure 3. Two-loop vertex and box graphs containing propagator-like pinch parts.

two-loop integrals. This reflects the fact that the pole position of the two-loop propagator is gauge independent. Note that for $p^2 = m_Z^2$ there is still a remaining gauge dependence in the function $g(A_0, B_0; \xi_W)$. It cancels with the gauge dependence of the terms generated by inserting one-loop counterterms into the one-loop diagrams.

3. GAUGE INVARIANCE OF TWO-LOOP SELF-ENERGIES

In order to investigate physical effects due to two-loop contributions of propagator type, it would be desirable to arrange these contributions in such a way that they form building blocks with suitable theoretical properties. At one-loop order, the pinch technique (PT) [7] was developed to eliminate the gauge parameter dependence by shifting contributions between different Green functions. It was found that the new “Green functions” obtained in this way fulfill simple Ward identities and in comparison to their R_ξ -gauge counterparts possess desirable properties such as improved IR and UV properties and a decent high-energy behavior.

However, it was recently shown [8] that the requirement of gauge parameter independence is not the crucial criterion for obtaining well-behaved Green functions. The background-field method (BFM) provides a more general framework in which the Green functions are directly derived from a gauge invariant effective action. Their desirable theoretical properties are a consequence of gauge invariance and hold for all values of the quantum gauge parameter ξ_Q . In [8] the BFM was applied to QCD and the SM. It was shown that the BFM includes the PT results as the special case $\xi_Q = 1$. Viewed from the framework of the BFM, the PT results therefore are not gauge independent but correspond to a cer-

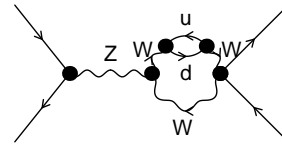


Figure 4. The pinch part of the first diagram in fig. 3.

tain choice of the quantum gauge parameter ξ_Q .

In order to discuss this issue at the two-loop level, we present here for an example the application of both approaches. In contrast to the BFM, the PT has so far been restricted to the one-loop level only. We therefore work out an extension to the two-loop case. We treat the “charged current” light fermion contributions to the two-loop Z self-energy. The result in the R_ξ gauge was given in (16).

3.1. Pinch technique at the two-loop level

In the PT, the gauge parameter dependence of self-energies is canceled by combining them with propagator-like pieces extracted from vertex and box diagrams which contribute to a gauge independent S-matrix element. The relevant types of two-loop vertex (containing also the wave function corrections) and box diagrams for a four-fermion process are drawn in fig. 3.

Parts of these vertex and box graphs in which the propagators of the external fermions have been canceled become propagator-like. Such a “pinch part” is depicted in fig. 4. It corresponds to the first diagram in fig. 3, in which the propagator associated with the final state fermions has been removed. The precise definition of the pinch parts a priori is not unique. In analogy to the one-loop case, we identify the pinch parts as terms emerging when a longitudinal momentum k_μ of an elementary vertex or propagator is contracted

with a coupling matrix γ^μ of the external fermion current. This gives rise to an elementary Ward identity, i.e. it can be written in terms of inverse fermion propagators and mass terms

$$k_\mu \gamma^\mu = (\not{p}_f + \not{k} - m_1) - (\not{p}_f - m_2) + m_1 - m_2, \quad (18)$$

where p_f is the momentum of the external fermion. The first term on the right-hand side cancels the fermion propagator and therefore gives rise to the pinch part, whereas on-shell the other terms yield contributions proportional to the fermion masses.

The k_μ -terms originate from the longitudinal part of the gauge boson propagators in the R_ξ -gauge (see (14)) and from the three-gauge-boson vertices. Up to group theoretical factors these vertices can be decomposed into

$$\begin{aligned} \Gamma_{\mu\nu\alpha} &= \Gamma_{\mu\nu\alpha}^P + \Gamma_{\mu\nu\alpha}^F, \quad \text{where} \\ \Gamma_{\mu\nu\alpha}^P &= (q+k)_\nu g_{\mu\alpha} + k_\mu g_{\nu\alpha}, \\ \Gamma_{\mu\nu\alpha}^F &= 2q_\mu g_{\nu\alpha} - 2q_\nu g_{\mu\alpha} - (2k+q)_\alpha g_{\mu\nu}. \end{aligned} \quad (19)$$

The momenta $(q+k)_\nu$ and k_μ in $\Gamma_{\mu\nu\alpha}^P$ have the same form as those arising from the longitudinal part of the relevant gauge boson propagators. Therefore $\Gamma_{\mu\nu\alpha}^P$ also gives rise to pinch parts. Note that in the first diagram of fig. 3 only the part of $\Gamma_{\mu\nu\alpha}^P$ directly acting on the external fermion line yields a pinch part.

Extracting the pinch parts of the diagrams represented by fig. 3 and combining them with the usual self-energy we find a result of the form

$$\begin{aligned} \Sigma_T^{R_\xi, (2)}(p^2) + \Sigma_{T, Pin}^{(2)}(p^2) &= \\ &= e^4 \left(\tilde{f}(A_0, B_0) + \tilde{g}(A_0, B_0; \xi_W) + \tilde{F}(T) \right). \end{aligned} \quad (20)$$

Here $\Sigma_T^{R_\xi, (2)}(p^2)$ denotes the usual self-energy in the R_ξ -gauge as given in (16), $\Sigma_{T, Pin}^{(2)}(p^2)$ are the pinch parts of the one-particle irreducible two-loop triangle and box graphs, $\tilde{f}(A_0, B_0)$ and $\tilde{F}(T)$ are gauge independent functions of scalar one-loop and two-loop integrals, respectively, whereas $\tilde{g}(A_0, B_0; \xi_W)$ still depends on the gauge parameter. This means that only the gauge parameter dependence of the terms containing the scalar two-loop integrals has disappeared, while the contributions involving the one-loop integrals remain

gauge dependent. This feature was in fact anticipated from the structure of the result (16). Since the pinch parts extracted from the two-loop triangle and box graphs are by construction proportional to $(p^2 - m_Z^2)$, they cannot cancel the gauge dependence still present in (16) for $p^2 = m_Z^2$.

The complete two-loop contribution to the gauge boson propagators in the PT is given as

$$\begin{aligned} \Delta_T^{PT, (2)}(p^2) &= -i \left\{ \frac{\Sigma_T^{R_\xi, (2)}(p^2) + \Sigma_{T, Pin}^{(2)}(p^2)}{(p^2 - m^2)^2} \right. \\ &\quad \left. - \frac{\left(\Sigma_T^{R_\xi, (1)}(p^2) + \tilde{\Sigma}_{T, Pin}^{(1)}(p^2) \right)^2}{(p^2 - m^2)^3} \right\}, \end{aligned} \quad (21)$$

where the first line contains the one-particle irreducible contributions of (20) and the second line the reducible ones. For the Z propagator one also has to take into account the mixing with the photon. Since $\tilde{\Sigma}_{T, Pin}^{(1)}(p^2)$ originates only from reducible graphs, it is not the full one-loop pinch part. In particular, it contains no contributions from one-loop box diagrams. However, these are necessary to cancel the gauge parameter dependence of the one-loop gauge boson self-energy, $\Sigma_T^{R_\xi, (1)}(p^2)$ [7]. The reducible contribution in (21) is therefore also gauge parameter dependent and does not correspond to the one-loop self-energy in the PT, $\Sigma_T^{PT, (1)}$.

To identify the quantity which has to be regarded as the two-loop self-energy in the PT framework, we write the propagator (21) as

$$\Delta_T^{PT, (2)}(p^2) = -i \left\{ \frac{\Sigma_T^{PT, (2)}}{(p^2 - m^2)^2} - \frac{(\Sigma_T^{PT, (1)})^2}{(p^2 - m^2)^3} \right\}.$$

This yields

$$\begin{aligned} \Sigma_T^{PT, (2)}(p^2) &= \Sigma_T^{R_\xi, (2)}(p^2) + \Sigma_{T, Pin}^{(2)}(p^2) \\ &\quad - \frac{1}{p^2 - m^2} \left[\left(\Sigma_T^{R_\xi, (1)}(p^2) + \tilde{\Sigma}_{T, Pin}^{(1)}(p^2) \right)^2 \right. \\ &\quad \left. - \left(\Sigma_T^{PT, (1)}(p^2) \right)^2 \right]. \end{aligned} \quad (22)$$

The two-loop self-energy constructed via the PT therefore involves both one-particle irreducible and reducible contributions.

We have evaluated this quantity for the ‘‘charged current’’ light fermion contributions to

the Z self-energy and found that it is in fact independent of the gauge parameters. The result will be given in the next section.

3.2. The background-field method

The BFM [9] is a technique for quantizing gauge theories without losing explicit gauge invariance. This is achieved by decomposing in the Lagrangian the usual gauge field into a background field \hat{V} and a quantum field V . By adding a suitable non-linear gauge-fixing term, an effective action $\Gamma[\hat{V}]$ is obtained which is invariant under gauge transformations of the background fields. While the background fields are associated with the tree propagators, the quantum fields appear only inside loops. In $\Gamma[\hat{V}]$, only for the quantum fields a gauge fixing is needed. We specify it by the quantum gauge parameter ξ_Q .

The BFM is valid for all vertex functions to all orders of perturbation theory. Its approach is very different from the PT. While the PT seeks to obtain suitable ‘‘Green functions’’ by eliminating their dependence on the parameters of the R_ξ -gauge, the BFM is based on the gauge invariance inherent in $\Gamma[\hat{V}]$. The fact that the vertex functions fulfill simple Ward identities and possess other desirable features is a direct consequence of gauge invariance in the BFM [8], whereas the PT provides no explanation for these properties.

The comparison of these methods at the two-loop level clearly shows the power of the BFM approach. In the PT an involved rearrangement was necessary between different Green functions contributing to a specific two-loop process and between reducible and irreducible contributions. Contrarily, the vertex functions of the BFM are uniquely given in terms of Feynman rules. One simply has to calculate the ‘‘charged current’’ diagrams shown in fig. 2b using the BFM Feynman rules. The result is just an ordinary self-energy which is guaranteed to be process independent. For the special case $\xi_Q = 1$ it reads

$$\begin{aligned} \Sigma_{T,\xi_Q=1}^{BFM,(2)}(p^2) &= \Sigma_{T,\xi=1}^{R_\xi,(2)}(p^2) - e^4 18 c_W^2 C \\ &\times \left[4(1-D)p^2 B_0(p^2; 0, 0) B_0(p^2; m_W^2, m_W^2) \right. \\ &\left. + (p^2 - m_Z^2) \left(\frac{(3-D)p^2 - m_W^2}{p^2 m_W^2} T_{13'4'}(m_W^2) \right) \right] \end{aligned}$$

$$\begin{aligned} &+ \frac{1}{p^2} T_{23'4'}(p^2; m_W^2) \\ &- 2(3-2D) T_{123'4'}(p^2; m_W^2, m_W^2) \\ &+ [p^2 - 4(2-D)m_W^2] \\ &\times T_{1123'4'}(p^2; m_W^2, m_W^2, m_W^2) \Big], \quad (23) \end{aligned}$$

where $\Sigma_{T,\xi=1}^{R_\xi,(2)}(p^2)$ is the conventional self-energy in the ‘t Hooft-Feynman gauge, i.e. the result given in (16) with $\xi_W = 1$. The result (23) exactly coincides with the PT expression (22). Therefore we find here the same connection between the PT and the BFM as in one-loop order, i.e. the BFM contains the PT results as a special case.

We would like to stress that the case $\xi_Q = 1$ displayed here is not distinguished in the BFM. All properties derivable from the gauge invariant effective action, e.g. the simple BFM Ward identities, hold for all finite values of ξ_Q . As an example, we list a Ward identity valid for the Z self-energy in the BFM to all orders

$$p^\mu \Sigma_{\mu\nu}^{\hat{Z}\hat{Z}}(p) - i M_Z \Sigma_\nu^{\hat{Z}\hat{Z}}(p) = 0, \quad (24)$$

where the conventions of [8] are used. We checked the validity of this Ward identity at the two-loop level by explicit computation for arbitrary ξ_Q . The Ward identity fulfilled by the conventional two-loop Z self-energy was given in [6]. It involves in addition the self-energy of the unphysical scalar χ and reducible contributions.

In analogy to the one-loop case, this means that the special case singled out in the PT is not unique. When studying applications of two-loop self-energies, it has to be investigated whether these are influenced by the ambiguity corresponding to different choices of ξ_Q .

4. ANALYTIC APPROACHES AND HYPERGEOMETRIC FUNCTIONS

4.1. Introductory remarks

As explained above, the algebraic reduction of two-loop self-energies leads to four types of two-loop scalar integrals, T_{234} , T_{1234} , T_{12345} and T_{134} . The last integral follows from T_{234} by setting $p^2 = 0$ (see below), so one needs to study three scalar two-loop integrals. For convenience, we will in the following relabel the integral T_{234}

as $T_{123}(p^2; m_1^2, m_2^2, m_3^2)$.

In this section we discuss analytic results in an arbitrary number of dimensions D for these integrals. They will be in the form of generalized hypergeometric functions, that is multiple series of ratios of p^2 and the masses. We also discuss the expansion of these results around $D = 4$. Only in those cases which fulfill the condition

$$p^2 m_1^2 m_2^2 m_3^2 \prod (p^2 - (m_1 \pm m_2 \pm m_3)^2) = 0 \quad (25)$$

for the three-particle cuts, the finite part can be expressed in terms of polylogarithms. A typical example is given below:

$$\begin{aligned} T_{123}(p^2; 0, 0, m^2) &= -m^2 \left(\frac{m^2}{4\pi\mu^2} \right)^{-2\delta} \\ &= \frac{\Gamma^2(1-\delta)\Gamma(\delta)\Gamma(-1+2\delta)}{\Gamma(2-\delta)} {}_2F_1(\delta, 2\delta-1; 2-\delta; z) \\ &= m^2 \left[\frac{1}{2\delta^2} + \frac{1}{\delta} \left(\frac{3}{2} - L_m - \frac{z}{4} \right) + 3 + \frac{3}{2}\zeta(2) \right. \\ &\quad \left. + L_m^2 - \left(3 - \frac{z}{2} \right) L_m - \frac{13}{8}z + Li_2(z) \right. \\ &\quad \left. - \frac{1}{2} \left(\frac{1}{z} - z \right) \log(1-z) \right] \quad (26) \end{aligned}$$

where $z = p^2/m^2$, $L_m = \gamma + \ln(m^2/4\pi\mu^2)$, γ is the Euler constant and $\zeta(2) = \pi^2/6$. Another example is the massive vacuum diagram $T_{123}(0; m_1^2, m_2^2, m_3^2)$ which in D dimensions is given in terms of four Appell F_4 functions but in four dimensions contains only dilogarithms [13]. In these specific cases one works with Feynman parameters or dispersion relations [14]. In the general mass case it turns out that x -space techniques and in particular the Mellin-Barnes representations are also useful. In the following subsections we will give an example of the application of dispersion relations and of the Mellin-Barnes representation.

4.2. The integral T_{123}

Let us first start with the rederivation of the so-called London transport diagram $T_{123}(p^2; m_1^2, m_2^2, m_3^2)$ by means of dispersion relations. The imaginary part or the discontinuity ΔT_{123} is given by

$$Im T_{123}(p^2; m_1^2, m_2^2, m_3^2) = \quad (27)$$

$$\begin{aligned} &\frac{\Delta T_{123}(p^2; m_1^2, m_2^2, m_3^2)}{2i} = \\ &-\pi(4\pi\mu^2)^{2\delta} \frac{\Gamma^2(1-\delta)}{\Gamma^2(2-2\delta)} \Theta(p^2 - (m_1 + m_2 + m_3)^2) \\ &\int_{(m_2+m_3)^2}^{(\sqrt{p^2}-m_1)^2} ds \frac{\lambda^{\frac{1}{2}-\delta}(s, m_2^2, m_3^2)}{s^{1-\delta}} \frac{\lambda^{\frac{1}{2}-\delta}(p^2, s, m_1^2)}{(p^2)^{1-\delta}} \\ &= \frac{1}{4\pi} \int_{(m_2+m_3)^2}^{(\sqrt{p^2}-m_1)^2} ds \Delta B_0(s; m_2^2, m_3^2) \Delta B_0(p^2; s, m_1^2) \end{aligned}$$

where $\lambda(a, b, c) = (a-b-c)^2 - 4bc$ is the Källén function. The dispersion relation reads

$$\begin{aligned} T_{123}(p^2; m_1^2, m_2^2, m_3^2) &= \\ &\frac{1}{2\pi i} \int_{(m_1+m_2+m_3)^2}^{\infty} dz \frac{1}{z-p^2} \Delta T_{123}(z; m_1^2, m_2^2, m_3^2) \\ &= \frac{1}{4\pi^2} \int_{(m_2+m_3)^2}^{\infty} ds \Delta B_0(s; m_2^2, m_3^2) \\ &\times \int_{(\sqrt{s+m_1})^2}^{\infty} \frac{dz}{z-p^2} \Delta B_0(z; s, m_1^2). \quad (28) \end{aligned}$$

Using the expansion

$$\frac{1}{z-p^2} = \frac{1}{z} \sum_{k=0}^{\infty} \left(\frac{p^2}{z} \right)^k \quad (29)$$

we perform first the integration over z :

$$\begin{aligned} A &= \sum_{k=0}^{\infty} (p^2)^k \int_u^{\infty} \frac{dz}{z^{k+2-\delta}} (z-u)^{1/2-\delta} (z-v)^{1/2-\delta} \\ &= \sum_{k=0}^{\infty} (p^2)^k u^{-\delta-k} B(k+\delta, 3/2-\delta) \\ &\times {}_2F_1(\delta-1/2, k+\delta; k+3/2; v/u) \quad (30) \end{aligned}$$

where $u = (m_1 + \sqrt{s})^2$ and $v = (m_1 - \sqrt{s})^2$. One can transform the Gauss hypergeometric function ${}_2F_1$ using relations which one can find in [15] leading to $T_{123}(p^2; m_1^2, m_2^2, m_3^2)$

$$T_{123}(p^2; m_1^2, m_2^2, m_3^2) = - (4\pi\mu^2)^\delta$$

$$\begin{aligned} & \times \frac{\Gamma(1-\delta)\Gamma(\delta-1)}{\Gamma(2-2\delta)} \int_{(m_2+m_3)^2}^{\infty} ds s^{\delta-1} \lambda^{\frac{1}{2}-\delta}(s, m_2^2, m_3^2) \\ & \left[\frac{m_1^2}{s} \left(\frac{m_1^2}{4\pi\mu^2} \right)^{-\delta} F_4(1, 2-\delta; 2-\delta, 2-\delta; \frac{p^2}{s}, \frac{m_1^2}{s}) \right. \\ & \quad \left. - \left(\frac{s}{4\pi\mu^2} \right)^{-\delta} F_4(1, \delta; 2-\delta, \delta; \frac{p^2}{s}, \frac{m_1^2}{s}) \right]. \quad (31) \end{aligned}$$

Since in (28) the z integration up to some factors represents the one-loop self-energy, we find as a byproduct

$$\begin{aligned} B_0(p^2; m_1^2, m_2^2) &= \Gamma(\delta-1) \\ & \times \left[\frac{m_1^2}{m_2^2} \left(\frac{m_1^2}{4\pi\mu^2} \right)^{-\delta} F_4(1, 2-\delta; 2-\delta, 2-\delta; \frac{p^2}{m_2^2}, \frac{m_1^2}{m_2^2}) \right. \\ & \quad \left. - \left(\frac{m_2^2}{4\pi\mu^2} \right)^{-\delta} F_4(1, \delta; 2-\delta, \delta; \frac{p^2}{m_2^2}, \frac{m_1^2}{m_2^2}) \right]. \quad (32) \end{aligned}$$

Using the definition of the F_4 functions we can easily perform the integration over s . After some manipulations we obtain the result for the London transport diagram which agrees with the one derived using x -space technique and Mellin-Barnes representation [16]. The result is presented in table (1), where $z_i = m_i^2/m_3^2$, $i = 1, 2$, $z_3 = p^2/m_3^2$ and $\nu = 1 - \delta$.

In the result we recognize a special instance of the Lauricella functions [17] defined by

$$F_C^{(n)}(a, b; c_1, \dots, c_n; z_1, \dots, z_n) = \sum_{k_1, \dots, k_n=0}^{\infty} \frac{(a)_{k_1+\dots+k_n} (b)_{k_1+\dots+k_n} z_1^{k_1} \dots z_n^{k_n}}{(c_1)_{k_1} \dots (c_n)_{k_n} k_1! \dots k_n!}, \quad (33)$$

where $(a)_k = \Gamma(a+k)/\Gamma(a)$. The defining multiple series converges for

$$\sqrt{|z_1|} + \dots + \sqrt{|z_n|} < 1. \quad (34)$$

The individual series above converge for $m_1 + m_2 + \sqrt{|p^2|} < m_3$. Collecting powers in p^2 , however, the total sum converges due to analyticity up to the next singularity on the physical sheet given by the threshold condition

$$|p^2| < (m_1 + m_2 + m_3)^2, \quad (35)$$

provided that the coefficients themselves do exist, which is the case for

$$m_1 + m_2 < m_3. \quad (36)$$

A Lauricella function in the arguments z_i for $i = 1, \dots, n$ can be analytically continued to a sum of two Lauricella functions in the arguments $x_i = z_i/z_n$ for $i = 1, \dots, n-1$ and $x_n = 1/z_n$ by the following relation [17]

$$F_C^{(n)}(a, b; c_1, \dots, c_n; z_1, \dots, z_n) = \quad (37)$$

$$f_1 F_C^{(n)}(a, 1+a-c_n; c_1, \dots, c_{n-1}, 1-b+a; x_1, \dots, x_n) + f_2 F_C^{(n)}(b, 1+b-c_n; c_1, \dots, c_{n-1}, 1-a+b; x_1, \dots, x_n).$$

where

$$\begin{aligned} f_1 &= \frac{\Gamma(c_n)\Gamma(b-a)}{\Gamma(b)\Gamma(c_n-a)} (-z_n)^{-a}, \\ f_2 &= \frac{\Gamma(c_n)\Gamma(a-b)}{\Gamma(a)\Gamma(c_n-b)} (-z_n)^{-b}. \end{aligned} \quad (38)$$

Applied to tab. (1) this yields, as one coefficient vanishes, a total of seven transformed Lauricella functions, which is also given in the tab. (2). Now, this expression is valid for

$$|p^2| > (m_1 + m_2 + m_3)^2. \quad (39)$$

One may wonder what the relation is between the large p^2 expansion of tab. (2) and that given in [18]. In the latter approach the various terms in the p^2 expansion are obtained from the expansion of subgraphs. The subgraphs are obtained by distributing the momentum p over the propagators in all possible ways. In the case of the London transport diagram one has the following subgraphs: the diagram itself, the three diagrams where one internal line is removed and the three diagrams where two internal lines have been removed.

Following the analysis of [18] one can easily find the first term of each of the contributing series. For the subgraph representing the whole diagram the first term in the series should be the massless diagram. This series then corresponds to the last term in tab. (2). The series which originates from the subgraph where two lines have been removed, e.g. 1 and 2, starts with the product of two massive tadpoles. They contribute a factor $(m_1^2 m_2^2)^\nu$ which can be identified with the third term in tab. (2). The remaining subgraphs are obtained by removing one internal line, e.g. line 3. This yields a series starting with a massive tadpole proportional to $(m_3^2)^\nu$. This is the sixth term

Table 1

The small p^2 result

$$\begin{aligned}
T_{123}(p^2; m_1^2, m_2^2, m_3^2) &= -m_3^2 \left(\frac{m_3^2}{4\pi\mu^2} \right)^{2(\nu-1)} \times \\
&\left\{ z_1^\nu z_2^\nu \Gamma^2(-\nu) F_C^{(3)}(1, 1 + \nu; 1 + \nu, 1 + \nu, 1 + \nu; z_1, z_2, z_3) \right. \\
&- z_1^\nu \Gamma^2(-\nu) F_C^{(3)}(1, 1 - \nu; 1 + \nu, 1 - \nu, 1 + \nu; z_1, z_2, z_3) \\
&- z_2^\nu \Gamma^2(-\nu) F_C^{(3)}(1, 1 - \nu; 1 - \nu, 1 + \nu, 1 + \nu; z_1, z_2, z_3) \\
&\left. - \Gamma(\nu)\Gamma(-\nu)\Gamma(1 - 2\nu) F_C^{(3)}(1 - 2\nu, 1 - \nu; 1 - \nu, 1 - \nu, 1 + \nu; z_1, z_2, z_3) \right\}
\end{aligned}$$

Table 2

The large p^2 result

$$\begin{aligned}
T_{123}(p^2; m_1^2, m_2^2, m_3^2) &= - \left(\frac{-p^2}{4\pi\mu^2} \right)^{2\nu-2} (-p^2) \times \\
&\left\{ (-x_1)^\nu (-x_3)^\nu \Gamma^2(-\nu) F_C^{(3)}(1, 1 - \nu; 1 + \nu, 1 - \nu, 1 + \nu; x_1, x_2, x_3) \right. \\
&+ (-x_2)^\nu (-x_3)^\nu \Gamma^2(-\nu) F_C^{(3)}(1, 1 - \nu; 1 - \nu, 1 + \nu, 1 + \nu; x_1, x_2, x_3) \\
&+ (-x_1)^\nu (-x_2)^\nu \Gamma^2(-\nu) F_C^{(3)}(1, 1 - \nu; 1 + \nu, 1 + \nu, 1 - \nu; x_1, x_2, x_3) \\
&+ (-x_1)^\nu \frac{\Gamma^2(\nu)\Gamma(-\nu)\Gamma(1-\nu)}{\Gamma(2\nu)} F_C^{(3)}(1 - \nu, 1 - 2\nu; 1 + \nu, 1 - \nu, 1 - \nu; x_1, x_2, x_3) \\
&+ (-x_2)^\nu \frac{\Gamma^2(\nu)\Gamma(-\nu)\Gamma(1-\nu)}{\Gamma(2\nu)} F_C^{(3)}(1 - \nu, 1 - 2\nu; 1 - \nu, 1 + \nu, 1 - \nu; x_1, x_2, x_3) \\
&+ (-x_3)^\nu \frac{\Gamma^2(\nu)\Gamma(-\nu)\Gamma(1-\nu)}{\Gamma(2\nu)} F_C^{(3)}(1 - \nu, 1 - 2\nu; 1 - \nu, 1 - \nu, 1 + \nu; x_1, x_2, x_3) \\
&\left. + \frac{\Gamma^3(\nu)\Gamma(1-2\nu)}{\Gamma(3\nu)} F_C^{(3)}(1 - 3\nu, 1 - 2\nu; 1 - \nu, 1 - \nu, 1 - \nu; x_1, x_2, x_3) \right\}.
\end{aligned}$$

in tab. (2). Thus the seven series in tab. (2) can be related directly to the seven subgraphs which are required for the method of [18].

For the special case $p^2 = 0$, $F_C^{(3)}$ reduces to the Appell function F_4 and we recover the result in the literature [13] for the vacuum diagram. On the other hand taking $m_1 = m_2 = 0$ only one of the Lauricella functions remains and becomes a Gauss hypergeometric function ${}_2F_1$ giving the result

$$\begin{aligned}
T_{123}(p^2; 0, 0, m^2) &= m^2 \left(\frac{m^2}{4\pi\mu^2} \right)^{-2\delta} \\
&\Gamma(1-\delta)\Gamma(\delta-1)\Gamma(2\delta-1) {}_2F_1(2\delta-1, \delta; 2-\delta; z),
\end{aligned} \tag{40}$$

which is the same as (26).

In the following the general D dimensional expression for the 2-loop London transport diagram will be expanded in $\delta = (4 - D)/2 = 1 - \nu$ for small $|p^2|$.

The following combination [19] of the general massive case with massless cases is chosen in such a way that the infinite parts cancel

$$\begin{aligned}
T_{123N}(p^2; m_1^2, m_2^2, m_3^2) &= \\
T_{123}(p^2; m_1^2, m_2^2, m_3^2) &- T_{123}(p^2; m_1^2, 0, m_3^2) \\
-T_{123}(p^2; 0, m_2^2, m_3^2) &+ T_{123}(p^2; 0, 0, m_3^2).
\end{aligned} \tag{41}$$

It is this combination which will be calculated in two independent ways.

An analytic form is obtained by expansion of the Lauricella functions and their coefficients in δ , where the first and the second logarithmic derivatives of the Γ -function occur at integer arguments

$$\begin{aligned}
\psi(n+1) &= -\gamma + \sum_{k=1}^n \frac{1}{k}, \\
\psi'(n+1) &= \zeta(2) - \sum_{k=1}^n \frac{1}{k^2}.
\end{aligned} \tag{42}$$

The $1/\delta^2$ and $1/\delta$ terms indeed drop out in the result and a finite combination of various multiple series remains. A good check is provided by the cancellation of γ in this finite expression. For small $|p^2|$, i.e. the region $|p^2| < m_3^2$, one finds

$$\begin{aligned} & T_{123N}(p^2; m_1^2, m_2^2, m_3^2)/m_3^2 = \\ & - \sum_{m,n=1,k=0}^{\infty} \frac{(t-2)!(t-1)!}{(m-1)!m!(n-1)!n!(k+1)!k!} z_1^m z_2^n z_3^k \\ & \left[\{ \psi(t) + \psi(t-1) - \psi(m) - \psi(m+1) + \log(z_1) \} \right. \\ & \quad \times \{ \psi(t) + \psi(t-1) - \psi(n) - \psi(n+1) + \log(z_2) \} \\ & \quad \left. + \psi'(t) + \psi'(t-1) \right] \end{aligned} \quad (43)$$

with $t = m + n + k$.

4.3. The integral T_{1234}

With the dispersion method described above we derive the *small p^2 result* for T_{1234} in D dimensions. The discontinuity ΔT_{1234} is a sum of a two and a three-particle cut, which we denote by $\Delta T_{1234}^{(2)}$ and $\Delta T_{1234}^{(3)}$, respectively. The two-particle cut is given by

$$\begin{aligned} & \Delta T_{1234}^{(2)}(p^2; m_1^2, m_2^2, m_3^2, m_4^2) \\ & = \Delta B_0(p^2; m_1^2, m_2^2) B_0(m_1^2; m_3^2, m_4^2). \end{aligned} \quad (44)$$

Inserting this result in the dispersion integral gives

$$\begin{aligned} T_{1234}^{(2)}(p^2) & = \frac{1}{2\pi i} \int_{(m_1+m_2)^2}^{\infty} dz \frac{1}{z-p^2} \Delta T_{1234}^{(2)}(z) \\ & = B_0(p^2; m_1^2, m_2^2) B_0(m_1^2; m_3^2, m_4^2). \end{aligned}$$

The discontinuity $\Delta T_{1234}^{(3)}$ is related to the three particle-cut given in (27) but with an additional propagator and therefore we get the dispersion relation

$$\begin{aligned} & T_{1234}^{(3)}(p^2; m_i^2) = -(4\pi\mu^2)^{2\delta} \frac{\Gamma^2(1-\delta)}{\Gamma^2(2-2\delta)} \\ & \times \int_{(m_3+m_4)^2}^{\infty} ds \frac{\lambda^{\frac{1}{2}-\delta}(s, m_3^2, m_4^2)}{s^{1-\delta}(s-m_1^2-i\epsilon)} \int_{(\sqrt{s}+m_2)^2}^{\infty} dz \frac{\lambda^{\frac{1}{2}-\delta}(s, z, m_2^2)}{z^{1-\delta}(z-p^2)}. \end{aligned} \quad (45)$$

After performing the z integration we obtain:

$$\begin{aligned} & T_{1234}^{(3)}(p^2; m_i^2) = -(4\pi\mu^2)^{\delta} \frac{\Gamma(1-\delta)\Gamma(\delta-1)}{\Gamma(2-2\delta)} \\ & \times \int_{(m_3+m_4)^2}^{\infty} ds \frac{s^{\delta-1}}{s-m_1^2} \lambda^{\frac{1}{2}-\delta}(s, m_3^2, m_4^2) \\ & \times \left[\frac{m_2^2}{s} \left(\frac{m_2^2}{4\pi\mu^2} \right)^{-\delta} F_4(1, 2-\delta; 2-\delta, 2-\delta; \frac{p^2}{s}, \frac{m_2^2}{s}) \right. \\ & \quad \left. - \left(\frac{s}{4\pi\mu^2} \right)^{-\delta} F_4(1, \delta; 2-\delta, \delta; \frac{p^2}{s}, \frac{m_2^2}{s}) \right]. \end{aligned} \quad (46)$$

Expanding $(s-m_1^2)^{-1}$ in m_1^2/s and performing the integration over s one gets

$$\begin{aligned} & T_{1234}^{(3)}(p^2; m_i^2) = \frac{\Gamma(1-\delta)\Gamma(1+\delta)}{\delta} \left(\frac{m_4^2}{4\pi\mu^2} \right)^{-2\delta} \\ & \times \sum_{m,n,k,l=0}^{\infty} z_1^k z_2^n (1-z_3)^l z_4^m \\ & \times \frac{\Gamma(1+m+n)\Gamma(1+\delta+m+n+k+l)}{\Gamma(2-\delta+m)m!n!l!} \\ & \times \left(z_2^{1-\delta} \frac{\Gamma(2-\delta+m+n)\Gamma(2+m+n+k+l)}{\Gamma(2-\delta+n)\Gamma(2(m+n+k)+4+l)} \right. \\ & \quad \left. - \frac{\Gamma(\delta+m+n)\Gamma(2\delta+m+n+k+l)}{\Gamma(\delta+n)\Gamma(2(m+n+k)+2+2\delta+l)} \right). \end{aligned} \quad (47)$$

where $z_i = m_i^2/m_4^2$ with $i = 1, 2, 3$ and $z_4 = p^2/m_4^2$. Note that the contribution from the three-particle cut is written in terms of multiple series which are not Lauricella functions anymore but they belong to a special class of generalized hypergeometric functions. To our knowledge they have not been studied in the mathematical literature.

With these results T_{1234} becomes

$$\begin{aligned} & T_{1234}(p^2; m_i^2) = T_{1234}^{(3)}(p^2; m_i^2) \\ & + B_0(p^2; m_1^2, m_2^2) B_0(m_1^2; m_3^2, m_4^2). \end{aligned} \quad (48)$$

Since the analytic continuation of the above generalized hypergeometric functions is not known to us we use the Mellin-Barnes representation technique to derive the *large p^2 expansion*. In this method a massive propagator is represented

in the following way:

$$\frac{1}{(k^2 - m^2)^\alpha} = \frac{1}{\Gamma(\alpha)} \frac{1}{2\pi i} \int_{-i\infty}^{+i\infty} ds \frac{(-m^2)^s}{(k^2)^{\alpha+s}} \times \Gamma(-s)\Gamma(\alpha + s), \quad (49)$$

where the integration contour in the s plane must separate the series of poles of $\Gamma(-s)$ on the right from the series of poles of $\Gamma(s + \alpha)$ on the left. In the expression for T_{1234} we apply (49) with $\alpha = 1$ to all propagators, thereby relating the general massive case to the massless one, but with the propagators raised to arbitrary powers $1+s_1, 1+s_2, 1+s_3, 1+s_4$. The corresponding result is well-known, see e.g.[13]. Closing the integration contours in a way that the convergence is guaranteed we get seven quartic series each of which can again be identified with the subgraph analysis for large p^2 expansions in [18].

The general small p^2 result for T_{1234} can be expanded in δ . The following combination of the general massive case with a massless case is chosen in such a way that the infinite parts cancel [19]

$$T_{1234N}(p^2; m_1^2, m_2^2, m_3^2, m_4^2) = T_{1234}(p^2; m_1^2, m_2^2, m_3^2, m_4^2) - T_{1234}(p^2; m_1^2, m_2^2, 0, 0). \quad (50)$$

The result can be found in [20].

As an example of a special case of these general results we choose $m_2 = m_3 = 0$ and $m_1 = m_4 = m$. Eq. (47) gives

$$T_{1234}^{(3)}(p^2) = -\frac{\Gamma(\delta)\Gamma(2\delta)\Gamma(1-\delta)}{(1-\delta)(1-2\delta)} \left(\frac{m^2}{4\pi\mu^2}\right)^{-2\delta} \times {}_2F_1(2\delta, \delta; 2-\delta; x). \quad (51)$$

To this the contribution from the two-particle cut $B_0(p^2; m^2, 0)B_0(m^2; 0, m^2)$ should be added

$$T_{1234}^{(2)}(p^2) = \frac{\Gamma^2(1+\delta)}{\delta^2(1-\delta)(1-2\delta)} \left(\frac{m^2}{4\pi\mu^2}\right)^{-2\delta} \times {}_2F_1(1, \delta; 2-\delta; x). \quad (52)$$

Expanding in δ we get

$$T_{1234}(p^2; m^2, 0, 0, m^2) = \frac{1}{2\delta^2} + \frac{1}{2\delta} \left\{ 5 - 2L_m + 2 \left(\frac{1-x}{x}\right) \ln(1-x) \right\}$$

$$+ \frac{19}{2} - \frac{1}{2}\zeta(2) + L_m^2 - 5L_m - 2L_m \left(\frac{1-x}{x}\right) \ln(1-x) + 5 \left(\frac{1-x}{x}\right) \ln(1-x) - \left(\frac{1-x}{x}\right) \ln^2(1-x) - \frac{1}{x} Li_2(x). \quad (53)$$

We conclude this section with some remarks on the master diagram $T_{12345}(p^2)$ in arbitrary number of dimensions. This case turns out to pose problems. For instance when one wants to apply the Mellin-Barnes representation, one needs the massless master diagram with arbitrary powers for the propagators. This expression is not (yet) available in the literature, which is related to the fact that the structure of the master diagram is not anymore of a self-energy insertion type.

5. ANALYTIC APPROACHES AND ELLIPTIC INTEGRALS

In this section we inspect the imaginary parts of the London transport diagram T_{123} and of T_{1234} . It turns out that they can be calculated in four dimensions in terms of complete elliptic integrals. These are well known functions and thus the results are of analytic interest. Furthermore fast and precise algorithms for the calculation of the elliptic integrals are available. Therefore the results provide also an efficient way to calculate the imaginary parts numerically.

5.1. The imaginary part of the London transport diagram

As can be seen from (27) the imaginary part of T_{123} is finite in four dimensions and reads with a factorization of the Källén functions

$$Im(T_{123}(p^2; m_i^2)) = \frac{1}{2i} \Delta T_{123}(p^2, m_i^2) = -\frac{\pi}{p^2} \int_{x_2}^{x_3} \frac{dt}{t} \sqrt{(t-x_1)(t-x_2)} \times \sqrt{(x_3-t)(x_4-t)}, \quad (54)$$

with

$$x_1 = (m_1 - m_2)^2, \quad x_2 = (m_1 + m_2)^2, \\ x_3 = (p - m_3)^2, \quad x_4 = (p + m_3)^2, \\ x_1 \leq x_2 \leq x_3 \leq x_4.$$

The integration limits are zeros of the square roots, and thus (54) leads to complete elliptic integrals, defined by

$$\begin{aligned} K(x) &= \int_0^1 \frac{dt}{\sqrt{(1-t^2)(1-x^2t^2)}} \\ &= \frac{\pi}{2} {}_2F_1\left(-\frac{1}{2}, \frac{1}{2}, 1, x^2\right), \end{aligned} \quad (55)$$

$$\begin{aligned} E(x) &= \int_0^1 \frac{dt(1-x^2t^2)}{\sqrt{(1-t^2)(1-x^2t^2)}} \\ &= \frac{\pi}{2} {}_2F_1\left(\frac{1}{2}, \frac{1}{2}, 1, x^2\right), \end{aligned} \quad (56)$$

$$\begin{aligned} \Pi(c, x) &= \int_0^1 \frac{dt}{(1-ct^2)\sqrt{(1-t^2)(1-x^2t^2)}} \\ &= \frac{\pi}{2} F_1\left(\frac{1}{2}; 1, \frac{1}{2}; 1; c, x^2\right), \end{aligned} \quad (57)$$

with the Gauss hypergeometric function ${}_2F_1$ and the Appell function F_1 [17,21,22]. Reduction of (54) to the Legendre normal form of the elliptic integrals [23,24] by decomposition into partial fractions and partial integration yields after some algebra

$$\begin{aligned} \text{Im}(T_{123}(p^2; m_1^2, m_2^2, m_3^2)) &= \\ &= -\frac{\pi}{p^2} \left\{ c_1 K(\kappa) + c_2 E(\kappa) + c_3 \Pi\left(\frac{q_{-+}}{q_{--}}, \kappa\right) \right. \\ &\quad \left. + c_4 \Pi\left(\frac{(m_1 - m_2)^2 q_{-+}}{(m_1 + m_2)^2 q_{--}}, \kappa\right) \right\} \\ &\quad \times \Theta(p^2 - (m_1 + m_2 + m_3)^2), \end{aligned} \quad (58)$$

$$\begin{aligned} c_1 &= 4m_1 m_2 \sqrt{\frac{q_{--}}{q_{++}}} \\ &\quad \times \left\{ (p + m_3)^2 - m_3 p + m_1 m_2 \right\}, \\ c_2 &= \frac{m_1^2 + m_2^2 + m_3^2 + p^2}{2} \sqrt{q_{++} q_{--}}, \\ c_3 &= \frac{8m_1 m_2}{\sqrt{q_{++} q_{--}}} \left\{ (m_1^2 + m_2^2)(p^2 + m_3^2) \right. \\ &\quad \left. - 2m_1^2 m_2^2 - 2m_3^2 p^2 \right\}, \\ c_4 &= -\frac{8m_1 m_2 (p^2 - m_3^2)^2}{\sqrt{q_{++} q_{--}}}, \\ \kappa^2 &= \frac{q_{+-} q_{-+}}{q_{++} q_{--}}, \end{aligned}$$

with variables $q_{\pm\pm}$ corresponding to the physical and unphysical thresholds

$$q_{\pm\pm} := (p \pm m_3)^2 - (m_1 \pm m_2)^2. \quad (59)$$

This result is valid for all values of m_1^2, m_2^2 and m_3^2 . In special cases it leads to simpler formulae. For equal masses one gets

$$\begin{aligned} \text{Im}(T_{123}(p^2; m^2, m^2, m^2)) &= -\frac{\pi}{p^2} \sqrt{(p-m)(p+3m)} \\ &\quad \times \left\{ \frac{(p-m)(p^2+3m^2)}{2} E(\kappa) - 4m^2 p K(\kappa) \right\} \\ &\quad \times \Theta(p^2 - 9m^2), \end{aligned} \quad (60)$$

$$\text{with } \kappa^2 = \frac{(p+m)^3(p-3m)}{(p-m)^3(p+3m)}, \quad (61)$$

involving only complete elliptic integrals of the first and second kind, i.e. ${}_2F_1$ Gauss' hypergeometric functions. If at least one mass is zero, $\text{Im}(T_{123})$ reduces to logarithms.

5.2. The imaginary part of T_{1234}

The two-particle cut contribution to the discontinuity of T_{1234} was given in (44),

$$\begin{aligned} \Delta T_{1234}^{(2)}(p^2; m_1^2, m_2^2, m_3^2, m_4^2) &= \\ &= \Delta B_0(p^2; m_1^2, m_2^2) B_0(m_1^2; m_3^2, m_4^2). \end{aligned} \quad (62)$$

As a product of a one-loop self-energy integral and a one-loop self-energy discontinuity it is composed of elementary functions and gets a real part for

$$(m_3 + m_4)^2 < m_1^2 \text{ and } (m_1 + m_2)^2 < p^2. \quad (63)$$

The three particle cut contribution looks very similar to that of the London transport diagram. Only one more propagator $1/(t - m^2)$ has to be added in (54). The calculation yields

$$\begin{aligned} \Delta T_{1234}^{(3)}(p^2; m_1^2, m_2^2, m_3^2, m_4^2) &= \\ &= \frac{2\pi i}{p^2} \left\{ c_1 K(\kappa) + c_2 E(\kappa) + c_3 \Pi\left(\frac{q_{-+}}{q_{--}}, \kappa\right) \right. \\ &\quad + c_4 \Pi\left(\frac{(m_3 - m_4)^2 q_{-+}}{(m_3 + m_4)^2 q_{--}}, \kappa\right) \\ &\quad \left. + c_5 \Pi\left(\frac{m_1^2 - (m_3 - m_4)^2 q_{-+}}{m_1^2 - (m_3 + m_4)^2 q_{--}} - i\epsilon, \kappa\right) \right\} \end{aligned}$$

$$\begin{aligned}
& \times \Theta(p^2 - (m_2 + m_3 + m_4)^2), \quad (64) \\
c_1 &= 4m_3m_4\sqrt{\frac{q_{--}}{q_{++}}}, \quad c_2 = \sqrt{q_{++}q_{--}}, \\
c_3 &= \frac{8m_3m_4(p^2 - m_1^2 + m_2^2 + m_3^2 + m_4^2)}{\sqrt{q_{++}q_{--}}}, \\
c_4 &= -\frac{8m_3m_4(p^2 - m_2^2)^2}{m_1^2\sqrt{q_{++}q_{--}}}, \\
c_5 &= \frac{8m_3m_4\lambda(p^2, m_1^2, m_2^2)}{m_1^2\sqrt{q_{++}q_{--}}}, \\
\kappa^2 &= \frac{q_{+-}q_{-+}}{q_{++}q_{--}},
\end{aligned}$$

with

$$q_{\pm\pm} := (p \pm m_2)^2 - (m_3 \pm m_4)^2. \quad (65)$$

In the case (63) the characteristic c of the last Π -function in (64) is greater than 1,

$$c = \frac{m_1^2 - (m_3 - m_4)^2 q_{-+}}{m_1^2 - (m_3 + m_4)^2 q_{--}} > 1, \quad (66)$$

which requires an analytic continuation of that function. A comprehensive discussion of the analytic properties of the elliptic integrals can be found in [25]. The $i\epsilon$ -prescription in (64) ensures that $\Delta T_{1234}^{(3)}$ gets the correct real part, given through

$$\begin{aligned}
& \text{Im}(\Pi(c - i\epsilon, \kappa)) \\
&= \frac{1}{2i} (\Pi(c - i\epsilon, \kappa) - \Pi(c + i\epsilon, \kappa)) \\
&= -\frac{\pi}{2} \sqrt{\frac{c}{(c-1)(c-\kappa^2)}}. \quad (67)
\end{aligned}$$

This contribution cancels the real part of $\Delta T_{1234}^{(2)}$. Consequently ΔT_{1234} is always purely imaginary.

Numerical checks show the agreement of the results of (58) for $\text{Im}(T_{123})$ and of

$$\text{Im}(T_{1234}) = \frac{1}{2i} (\Delta T_{1234}^{(2)} + \Delta T_{1234}^{(3)}) \quad (68)$$

with previously published tables [16,19].

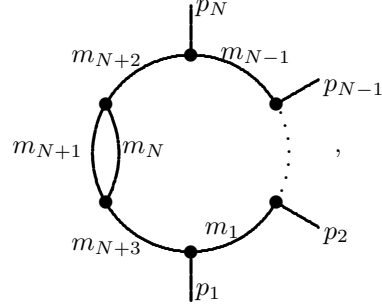
6. ONE-DIMENSIONAL INTEGRAL REPRESENTATIONS

6.1. A general approach to two-loop integrals containing a self-energy subloop

An alternative method to the series expansion of the two-loop scalar diagrams consists in

the derivation of one-dimensional integral representations. These are built up from one-loop self-energy functions B_0 coming from the self-energy subloop and the remaining one-loop integral. They can be derived by using a dispersion representation of the B_0 function.

A two-loop diagram with only three-vertices



where k is the momentum flowing through the self-energy insertion, can in a first step be reduced to simpler diagrams by a decomposition into partial fractions

$$\begin{aligned}
& \frac{1}{k^2 - m_{N+2}^2} \frac{1}{k^2 - m_{N+3}^2} = \frac{1}{m_{N+2}^2 - m_{N+3}^2} \\
& \times \left(\frac{1}{k^2 - m_{N+2}^2} - \frac{1}{k^2 - m_{N+3}^2} \right).
\end{aligned}$$

This results for the diagram in

$$\begin{aligned}
T_{1\dots N+3}(p_i; m_i^2) &= \frac{1}{m_{N+2}^2 - m_{N+3}^2} \\
& \times \left(T_{1\dots N+2}(p_i; m_1^2, \dots, m_{N+1}^2, m_{N+2}^2) \right. \\
& \left. - T_{1\dots N+2}(p_i; m_1^2, \dots, m_{N+1}^2, m_{N+3}^2) \right). \quad (69)
\end{aligned}$$

The difference has to be replaced by a derivative if $m_{N+2}^2 = m_{N+3}^2$.

Insertion of the dispersion representation for the self-energy subloop leads to

$$\begin{aligned}
& T_{1\dots N+2}(p_i; m_1^2, \dots, m_{N+1}^2, m_{N+2}^2) \\
&= \int d^D k B_0(k^2; m_N^2, m_{N+1}^2) \frac{1}{(k + p_1)^2 - m_1^2} \\
& \dots \times \frac{1}{(k + p_1 + \dots + p_{N-1})^2 - m_{N-1}^2} \\
& \times \frac{1}{k^2 - m_{N+2}^2}
\end{aligned}$$

$$\begin{aligned}
&= \frac{1}{2\pi i} \int_{s_0}^{\infty} ds \Delta B_0(s; m_N^2, m_{N+1}^2) \\
&\quad \times \int d^D k \frac{-1}{k^2 - s + i\epsilon} \frac{1}{k^2 - m_{N+2}^2} \\
&\quad \times \frac{1}{(k + p_1)^2 - m_1^2} \cdots \\
&\quad \times \frac{1}{(k + p_1 + \dots + p_{N-1})^2 - m_{N-1}^2}. \quad (70)
\end{aligned}$$

After a further decomposition into partial fractions,

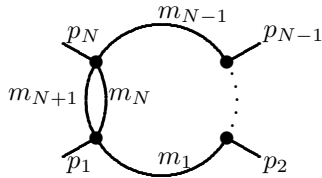
$$\begin{aligned}
&\frac{-1}{k^2 - s} \frac{1}{k^2 - m_{N+2}^2} \\
&= \frac{1}{s - m_{N+2}^2} \left(\frac{1}{k^2 - m_{N+2}^2} - \frac{1}{k^2 - s} \right), \quad (71)
\end{aligned}$$

the k -integrations and one of the s -integrations can be performed yielding

$$\begin{aligned}
&T_{1\dots N+2}(p_i; m_1^2, \dots, m_{N+1}^2, m_{N+2}^2) \\
&= B_0(m_{N+2}^2; m_N^2, m_{N+1}^2) \\
&\quad \times T^{(1)}(p_i; m_1^2, \dots, m_{N-1}^2, m_{N+2}^2) \\
&\quad - \frac{1}{2\pi i} \int_{s_0}^{\infty} ds \frac{\Delta B_0(s; m_N^2, m_{N+1}^2)}{s - m_{N+2}^2} \\
&\quad \times T^{(1)}(p_i; m_1^2, \dots, m_{N-1}^2, s). \quad (72)
\end{aligned}$$

$T^{(1)}$ denotes a one-loop N -point function in which s enters in the remaining one-dimensional integration as a mass variable.

A diagram with two four-vertices leads to a result which is similar to the remaining integration in (72),



$$\begin{aligned}
&T_{1\dots N+1}(p_i; m_i^2) \\
&= \frac{1}{2\pi i} \int_{s_0}^{\infty} ds \Delta B_0(s; m_N^2, m_{N+1}^2)
\end{aligned}$$

$$\begin{aligned}
&\times \int d^D k \frac{-1}{k^2 - s} \frac{1}{(k + p_1)^2 - m_1^2} \cdots \\
&\quad \times \frac{1}{(k + p_1 + \dots + p_{N-1})^2 - m_{N-1}^2} \\
&= -\frac{1}{2\pi i} \int_{s_0}^{\infty} ds \Delta B_0(s; m_N^2, m_{N+1}^2) \\
&\quad \times T^{(1)}(p_i; m_1^2, \dots, m_{N-1}^2, s). \quad (73)
\end{aligned}$$

As an example, we apply (72) to T_{1234} :

$$\begin{aligned}
&T_{1234}(p^2; m_1^2, m_2^2, m_3^2, m_4^2) \\
&= B_0(m_1^2; m_3^2, m_4^2) B_0(p^2; m_1^2, m_2^2) \\
&\quad - \frac{1}{2\pi i} \int_{(m_3+m_4)^2}^{\infty} ds \frac{\Delta B_0(s; m_3^2, m_4^2)}{s - m_1^2 + i\epsilon} \\
&\quad \times B_0(p^2; s, m_2^2). \quad (74)
\end{aligned}$$

An application of (73) to the London transport diagram leads to

$$\begin{aligned}
&T_{123} = -\frac{1}{2\pi i} \int_{(m_2+m_3)^2}^{\infty} ds \Delta B_0(s; m_2^2, m_3^2) \\
&\quad \times B_0(p^2; s, m_1^2), \quad (75)
\end{aligned}$$

a result which would also follow from (28).

The representations (75) and (74) with the subtractions (41) and (50) provide efficient ways to calculate T_{123N} and T_{1234N} in all parameter regions. The results agree numerically with those published in [16,19].

6.2. Integral representation of the master diagram

In this section a one-dimensional integral representation for the master diagram T_{12345} (fig. 1) in the general mass case is derived. This representation uses only elementary functions and is thus well suited for numerical evaluation.

We use the dispersion relation. The two-particle cut contributions are denoted $T^{(2a)}$ for the cut through the propagators 1 and 2, and $T^{(2b)}$ for the cut 4-5. The Cutkosky rules yield

$$\begin{aligned}
&\Delta T^{(2a)}(p^2; m_1^2, m_2^2, m_3^2, m_4^2, m_5^2) \\
&= \Delta B_0(p^2; m_1^2, m_2^2) \\
&\quad \times (C_0(p^2, m_1^2, m_2^2; m_4^2, m_3^2, m_5^2))^*. \quad (76)
\end{aligned}$$

This shows that the two-particle cut contributions are given by the self-energy discontinuity and the complex conjugate of the triangle diagram C_0 . For a further evaluation of (76) one can introduce the dispersion representation of C_0 ,

$$C_0(p_1^2, p_2^2, p_3^2; m_1^2, m_2^2, m_3^2) = \frac{1}{2\pi i} \int_{(m_1+m_2)^2}^{\infty} dt \frac{\Delta C_0(t)}{t - p_1^2 - i\epsilon} + C_{0an}, \quad (77)$$

with a contribution of the discontinuity belonging to the normal threshold

$$\begin{aligned} \Delta C_0(t, p_2^2, p_3^2; m_1^2, m_2^2, m_3^2) &= -\frac{2\pi i}{\sqrt{\lambda(t, p_2^2, p_3^2)}} \log \frac{a+b}{a-b} \\ a &= t(t + 2m_3^2 - p_2^2 - p_3^2 - m_1^2 - m_2^2) \\ &\quad + (p_3^2 - p_2^2)(m_1^2 - m_2^2), \\ b &= \sqrt{\lambda(t, p_2^2, p_3^2)} \sqrt{\lambda(t, m_1^2, m_2^2)}, \end{aligned} \quad (78)$$

and a contribution C_{0an} belonging to the anomalous threshold, resulting from the leading Landau singularity. This anomalous threshold at

$$\begin{aligned} t_1 &= m_3^2(-m_3^2 + p_2^2 + p_3^2 + m_1^2 + m_2^2) \\ &\quad - (p_2^2 - m_2^2)(p_3^2 - m_1^2) \\ &\quad - \sqrt{\lambda(p_2^2, m_2^2, m_3^2)} \sqrt{\lambda(p_3^2, m_1^2, m_2^2)} \end{aligned} \quad (79)$$

occurs if

$$\begin{aligned} m_1 p_2^2 + m_2 p_3^2 - m_3^2(m_1 + m_2) \\ - m_1 m_2(m_1 + m_2) > 0. \end{aligned} \quad (80)$$

Following the argument outlined in [26] one can show that its contribution is

$$C_{0an} = \int_{(m_1+m_2)^2}^{t_1} \frac{dt}{t - p_1^2} \frac{2\pi i}{\sqrt{\lambda(t, p_2^2, p_3^2)}} \quad (81)$$

and yields logarithms and square roots. In those cases, where t_1 is situated on the real axis and $t_1 > t_0 = (m_1 + m_2)^2$, this contribution can also be taken into account by choosing the appropriate sheets for the logarithm in (78).

After insertion of (77) into (76) the integrations in the dispersion integral can be interchanged and

lead to

$$\begin{aligned} T^{(2a)}(p^2; m_1^2, m_2^2, m_3^2, m_4^2, m_5^2) &= \frac{1}{2\pi i} \int_{s_0}^{\infty} \frac{ds}{s - p^2 - i\epsilon} \Delta T^{(2a)}(s; m_i^2) \\ &= \left(\frac{1}{2\pi i}\right)^2 \int_{t_0}^{\infty} dt \int_{s_0}^{\infty} ds \\ &\quad \times \frac{\Delta C_0(t) \Delta B_0(s)}{(s - p^2 - i\epsilon)(t - s + i\epsilon)} \\ &\quad + \frac{1}{2\pi i} \int_{s_0}^{\infty} ds \frac{\Delta B_0(s; m_1^2, m_2^2)}{s - p^2 - i\epsilon} \\ &\quad \times (C_{0an}(s, m_1^2, m_2^2; m_3^2, m_4^2, m_5^2))^* \\ &= \frac{1}{2\pi i} \int_{(m_4+m_5)^2}^{\infty} dt \frac{\Delta C_0(t, m_1^2, m_2^2; m_4^2, m_3^2, m_5^2)}{t - p^2 - i\epsilon} \\ &\quad \times (B_0(p^2; m_1^2, m_2^2) - B_0(t; m_1^2, m_2^2)) \\ &\quad + \frac{1}{2\pi i} \int_{(m_1+m_2)^2}^{\infty} ds \frac{\Delta B_0(s; m_1^2, m_2^2)}{s - p^2 - i\epsilon} \\ &\quad \times (C_{0an}(s, m_1^2, m_2^2; m_3^2, m_4^2, m_5^2))^*. \end{aligned} \quad (82)$$

To calculate the contribution of the other two-particle cut $\Delta T^{(2b)}$, the masses have to be interchanged according to $m_1 \leftrightarrow m_4$, $m_2 \leftrightarrow m_5$. Furthermore no complex conjugated form of C_0 has to be inserted in (76), resulting in a complex conjugated form of $B_0(t; m_4^2, m_5^2)$ in the first term of (82) and no complex conjugated form of C_{0an} in the second term of (82).

To evaluate the three-particle cut contributions, we keep close to Broadhurst's approach [27]. The contribution $T^{(3a)}$ refers to the cut 2-3-4, $T^{(3b)}$ refers to the cut 1-3-5. The Cutkosky rules yield

$$\begin{aligned} \Delta T^{(3a)}(p^2; m_1^2, m_2^2, m_3^2, m_4^2, m_5^2) &= -\frac{1}{2\pi i} \int_{(m_3+m_4)^2}^{(\sqrt{s}-m_2)^2} dt \frac{\Delta B_0(p^2; t, m_2^2)}{t - m_1^2 + i\epsilon} \\ &\quad \times \Delta C_0(t, p^2, m_2^2; m_3^2, m_4^2, m_5^2). \end{aligned} \quad (83)$$

A partial integration in (83) leads to a form which

simplifies the dispersion integral considerably

$$\begin{aligned}
T^{(3a)}(p^2; m_i^2) &= \\
&= \int_{s_0}^{\infty} ds \frac{\Delta T^{(3a)}(s; m_i^2)}{s - p^2 - i\epsilon} \\
&= \int_{(m_2+m_3+m_4)^2}^{\infty} \frac{ds}{s(s-p^2)} \\
&\quad \frac{(\sqrt{s-m_2})^2}{(m_3+m_4)^2} \\
&\quad \times \int_{(m_3+m_4)^2}^{\infty} dt \log \left(\frac{t}{m_1^2} - 1 + i\epsilon \right) \\
&\quad \times \sqrt{\lambda(s, t, m_2^2)} \\
&\quad \times R(s, t, m_2^2, m_3^2, m_4^2, m_5^2), \tag{84}
\end{aligned}$$

where R is for the case of different masses a rational function of s containing only first order poles. An interchange of integrations,

$$\begin{aligned}
&\int_{(m_2+m_3+m_4)^2}^{\infty} ds \int_{(m_3+m_4)^2}^{(\sqrt{s-m_2})^2} dt \\
&= \int_{(m_3+m_4)^2}^{\infty} dt \int_{(m_2+\sqrt{t})^2}^{\infty} ds, \tag{85}
\end{aligned}$$

and decomposition of $R(s)$ into partial fractions leads to integrations of the type

$$\begin{aligned}
&\int_{(\sqrt{t}+m_2)^2}^{\infty} \frac{ds}{s-s_i-i\epsilon} \frac{\sqrt{\lambda(s, t, m_2^2)}}{s} \\
&= B_0(s_i; t, m_2^2), \tag{86}
\end{aligned}$$

i.e. one-loop self-energy integrals. In the final expression all ultraviolet divergences of these B_0 -functions cancel. The result for the three-particle cut contribution of the master diagram is then

$$\begin{aligned}
T^{(3a)}(p^2; m_i^2) &= \\
&= \int_{(m_3+m_4)^2}^{\infty} dt \log \left(\frac{t}{m_1^2} - 1 + i\epsilon \right) \\
&\quad \times \frac{\sqrt{\lambda(t, m_4^2, m_3^2)}}{t m_3^2}
\end{aligned}$$

$$\times \sum_{i=1}^4 c_i \frac{B_0(p^2; t, m_2^2) - B_0(s_i; t, m_2^2)}{s_i^2 - p^2}, \tag{87}$$

with

$$\begin{aligned}
s_{1/2} &= \frac{t + m_2^2 + m_4^2 + m_5^2 - m_3^2}{2} \\
&\quad + \frac{(t - m_4^2)(m_5^2 - m_2^2)}{2m_3^2} \\
&\quad \pm \frac{\sqrt{\lambda(t, m_3^2, m_4^2)\lambda(m_2^2, m_3^2, m_5^2)}}{2m_3^2}, \\
s_{3/4} &= (m_2 \pm \sqrt{t})^2, \\
r_1 &= t(2m_2^2 - m_5^2 + m_3^2) - m_2^2(m_4^2 - m_3^2), \\
r_2 &= (t - m_2^2)(t(m_5^2 - m_3^2) - m_2^2(m_4^2 - m_3^2)), \\
r_3 &= \frac{m_3^2(m_3^2 - t - m_4^2)}{\lambda(t, m_4^2, m_3^2)}, \\
r_4 &= m_3^2
\end{aligned}$$

$$\begin{aligned}
&+ \left\{ t(2m_4^2 m_3^2 - m_4^2 m_2^2 + m_3^2 m_4^2 + m_5^2 m_3^2) \right. \\
&\quad + m_4^2(m_2^2 - m_5^2)(m_4^2 - m_3^2) \\
&\quad \left. + m_5^2 m_3^2(m_4^2 - m_3^2) \right\} \frac{1}{\lambda(t, m_4^2, m_3^2)},
\end{aligned}$$

$$c_1 = \left\{ s_1 r_1 + r_2 \right. \\
\left. + s_1(s_1^2 - (s_3 + s_4) - s_3 s_4)(s_1 r_3 - r_4) \right\}$$

$$\times \frac{1}{\prod_{i=2}^4 (s_1 - s_i)}, \quad c_2 = c_1(s_1 \leftrightarrow s_2),$$

$$c_4 = \frac{s_4 r_1 + r_2}{\prod_{i=1}^3 (s_4 - s_i)}, \quad c_3 = c_4(s_3 \leftrightarrow s_4).$$

Some special mass cases have to be considered: double poles occur in $R(s)$ if $m_2 = 0$ or if $\lambda(m_2^2, m_5^2, m_3^2) = 0$. The decomposition into partial fractions leads then to modified results involving functions

$$\begin{aligned}
&\int_{(\sqrt{t}+m_2)^2}^{\infty} \frac{ds}{(s-s_i^2-i\epsilon)^2} \frac{\sqrt{\lambda(s, t, m_2^2)}}{s} \\
&= \frac{\partial B_0(s_i, t, m_2^2)}{\partial s_i}. \tag{88}
\end{aligned}$$

Another modification of the decomposition into

partial fractions occurs if $m_3 = 0$, in which case the result is considerably simpler.

Broadhurst has evaluated the master diagram for some cases of physical interest [27]. They all belong to the special cases mentioned above, if the symmetries of the master diagram are exploited. The formulae (82) and (87) provide a method to calculate the master diagram in the general mass case. The occurring elementary one-dimensional integrations are numerically stable and the results agree with those of Kreimer's method [19]. Compared with the latter the one-dimensional integral representation is much faster, especially if high accuracy is required.

7. CONCLUSIONS

On the long way to complete two-loop calculations in the Standard Model this paper focuses on the self-energy diagrams.

When one restricts calculations to self-energies, these should be useful as building blocks with suitable theoretical properties. In particular, their gauge dependence has to be considered. We have discussed this problem for light fermionic contributions to the two-loop Z self-energy by applying two different approaches, the pinch technique (PT) and the background-field method (BFM). The PT aims on eliminating the gauge parameter dependence of Green functions within R_ξ -gauges, while in the BFM Green functions are derived from a gauge invariant effective action. Whereas the BFM is valid to all orders in perturbation theory, the PT had so far been restricted to the one-loop level.

In this paper an extension of the PT to the two-loop case has been worked out yielding (within R_ξ -gauges) a gauge parameter independent result. It involves a rearrangement of contributions between different Green functions and between one-particle irreducible and reducible diagrams. The BFM has been shown to provide a more general framework. Like at one-loop order, it incorporates the PT results as a special case. The BFM vertex functions fulfill simple Ward identities which are a direct consequence of gauge invariance. This holds for all values of the quantum gauge parameter ξ_Q .

For large parts of the actual calculation of the two-loop self-energy diagrams we use an algebraic approach allowing for a high degree of automatization. By applying a method for tensor integral decomposition, all two-loop self-energies are reduced to a minimal basis of standard scalar integrals.

The evaluation of the scalar diagrams is the remaining problem and is in essence more involved than in the case of one-loop diagrams. The reason is that for the general mass case needed in the SM functions beyond the usual (poly) logarithms are required. Analytic and numerical approaches have been discussed.

We have derived analytic results in terms of generalized hypergeometric functions for the scalar self-energy integrals with three and four propagators and arbitrary masses. This offers the possibility to use well-known mathematical techniques like analytic continuation, partial differential equations, or contour integral representations. The known formulas for integrals with vanishing masses are obtained as special cases and consequently are unified in one result in D dimensions. For the general mass case of the master diagram a representation in the form of a generalized hypergeometric function is not yet known.

When one is interested only in the imaginary parts, an alternative analytic result in four dimensions is obtained in terms of complete elliptic integrals. Since their properties are well-known they are easily accessible for numerical evaluations.

Finally, we have derived a one-dimensional integral representation for all two-loop diagrams containing a self-energy insertion. For the two-loop self-energy diagrams treated in this paper, the integrand is composed of elementary functions only and the representation is valid for all values of p^2 . Also for the master diagram a one-dimensional elementary integral representation is derived. The main application of these integrals is for numerical evaluations, giving a good alternative to the existing two-dimensional integrals.

Once adequate techniques for the self-energy diagrams are available, one could envisage practical applications for physics predictions. For the electroweak theory the obvious application is to

the gauge boson self-energies which play a role in the $M_W - M_Z$ mass relation and details of the Z line shape. For QED the two-loop vacuum polarization is known since a long time [28], but the electron two-loop self-energy was never fully calculated.

ACKNOWLEDGEMENTS

The authors would like to thank the organizers of the Teupitz meeting for the kind hospitality during the workshop. We also acknowledge fruitful discussions with our colleagues, especially with A. Denner, S. Dittmaier, R. Scharf and J.B. Tausk.

REFERENCES

1. A. Blondel, talk given at the *Zeuthen Workshop on Elementary Particle Theory*, Teupitz, (April 1994).
2. J. van der Bij and F. Hoogeveen, *Nucl. Phys.* B283 (1987) 477.
3. R. Barbieri, M. Beccaria, P. Ciafaloni, G. Curci and A. Vicere, *Phys. Lett.* B288 (1992) 95, *erratum*: B312 (1993) 511; *Nucl. Phys.* B409 (1993) 105.
4. J. van der Bij and M. Veltman, *Nucl. Phys.* B231 (1984) 205; J. van der Bij, *Nucl. Phys.* B248 (1984) 141.
5. G. Passarino and M. Veltman, *Nucl. Phys.* B160 (1979) 151.
6. G. Weiglein, R. Scharf and M. Böhm, *Nucl. Phys.* B416 (1994) 606.
7. J. Papavassiliou, *Phys. Rev.* D41 (1990) 3179; G. Degrossi and A. Sirlin, *Phys. Rev.* D46 (1992) 3104, and references therein.
8. A. Denner, S. Dittmaier and G. Weiglein, *Bielefeld preprint BI-TP. 94/17*, *hep-ph/9406204*, to appear in *Phys. Lett. B*; *Bielefeld preprint BI-TP. 94/22*, to appear in *Nucl. Phys. B* (Proceedings Supplements).
9. L.F. Abbott, *Nucl. Phys.* B185 (1981) 189; *Acta Phys. Pol.* B13 (1982) 33, and references therein.
10. J. Küblbeck, M. Böhm and A. Denner, *Comp. Phys. Comm.* 60 (1990) 165.
11. R. Mertig, M. Böhm and A. Denner, *Comp. Phys. Comm.* 64 (1991) 345.
12. G. Weiglein, R. Mertig, R. Scharf and M. Böhm, in *New Computing Techniques in Physics Research 2*, ed.: D. Perret-Gallix, World Scientific 1992, p. 617.
13. A.I. Davydychev, J.B. Tausk, *Nucl. Phys.* B 397 (1993) 123.
14. R. Scharf and J.B. Tausk, *Nucl. Phys.* B 412 (1994) 423
15. A.P. Prudnikov, Yu.A. Brychkov and O.I. Marichev, *Integrals and Series*, Gordon and Breach Science Publishers, New York (1986).
16. F.A. Berends, M. Buza, M. Böhm and R. Scharf, *Leiden preprint INLO-PUB-17/93*, to appear in *Z. Phys.*
17. H. Exton, *Multiple Hypergeometric Functions and Applications*, Ellis Horwood Limited, Chichester (1976).
18. A.I. Davydychev, V.A. Smirnov and J.B. Tausk, *Nucl. Phys.* B 410 (1993) 325.
19. F.A. Berends and J.B. Tausk, *Leiden preprint INLO-PUB-15/93*, to appear in *Nucl. Phys. B*.
20. S. Bauberger, F.A. Berends, M. Böhm and M. Buza, *Leiden preprint INLO-PUB-9/94*
21. P. Appell, J. Kampé de Fériet, *Fonctions Hypergéométriques*, Gauthier-Villars, Paris (1926).
22. H.M. Srivastava, P.W. Karlson, *Multiple Gaussian Hypergeometric Series*, Halstead Press, John Wiley, New York (1985)
23. A. Erdélyi, W. Magnus, F. Oberhettinger, F.G. Tricomi, *Higher Transcendental Functions*, vol. II, McGraw-Hill, New York (1953).
24. M. Abramowitz, I.A. Stegun, *Handbook of Mathematical Functions*, Dover Publications, New York (1972).
25. F. Tricomi, M. Krafft, *Elliptische Funktionen*, Akademische Verlagsgesellschaft, Leipzig (1948). ITAL: Funzioni ellittiche.
26. G. Barton, *Introduction to Dispersion Techniques in Field Theory*, Benjamin, New York (1965).
27. D.J. Broadhurst, *Z.Phys.*, C 47 (1990) 115.
28. G. Källén, A. Sabry, *Dan. Met. Fys. Medd.*, 29 (1955) no. 17